Estimating the density of Florida panthers using camera traps and telemetry – Report for Phase 2 of the project

Robert M. Dorazio, Research Statistician, U.S. Geological Survey, Wetland and Aquatic Research Center, 7920 NW 71st Street, Gainesville, FL 32653, Phone: (352) 264-3476, Fax: (352) 378-4956, Email: bdorazio@usgs.gov.

Dave Onorato, Associate Research Scientist, Florida Fish and Wildlife Conservation Commission, Fish and Wildlife Research Institute, 298 Sabal Palm Road, Naples, FL 34114, Phone: (239) 417-6352, Fax: (239) 417-6361, Email: dave.onorato@myfwc.com.

1 INTRODUCTION

In Phase 2 of this project we planned to develop a statistical model that could be used to compute a population-wide estimate of Florida panther abundance. Specifically, we intended to extend the statistical model of Sollmann et al. (2013b) to include the effects of habitat on the movements and home ranges of individual panthers. This approach, while ambitious, offers the advantage of using additional information about habitat to improve the accuracy of abundance estimates in both surveyed and unsurveyed study areas. For example, panthers likely select home ranges based on suitable habitat (e.g., adequate abundance of prey), whereas other aspects of the habitat, such as presence of trails and roads, may influence a panther's movements. The success of this modeling approach depends on the extent to which suitable measures of habitat can be identified over the entire region occupied by panthers. Potential habitat covariates include hydrologic measurements (as surrogates of flooding), recreational hunting use (as a categorical indicator of prey abundance), and presence of trails and roads. Our goal was to add biological realism to the statistical model for the purpose of obtaining more accurate and precise estimates of panther abundance over the current breeding range.

A secondary goal of our efforts was to formulate the observational component of the statistical model of panther detections more accurately. In the model of Sollmann et al. (2013b) the entire survey period was partitioned into a finite number of non-overlapping time periods (months) because the exact time and date of photographic "captures" were not always recorded owing to camera failure. However, in the absence of camera failures, the time and date of each observation need not be assigned into a discrete time period. These assignments are subjective and can lead to loss of information in the detection process. Therefore, we planned to formulate models of the exact times of panther detections using a continuous-time stochastic process to specify the detections of panthers in camera traps.

At a conceptual level, our efforts were intended to provide a coherent analytical framework that would be applicable across the following spectrum of sampling situations:

$$\text{Marked population} \iff \text{Partially marked population} \iff \text{Unmarked population}$$

At one end of this spectrum is the analysis of detections of completely *marked* individuals (e.g., individual tigers identified by their unique body stripe patterns). For example, Dorazio and Karanth (2017) developed a continuous-time, spatial capture-recapture (SCR) model to analyze the detections of marked individuals. This model included the following components:

- number and spatial distribution of individual activity centers (home range centroids) were specified in terms of one or more spatially varying covariates (e.g., measures of habitat or prey

abundance)

- number and spatio-temporal distribution of detection times were specified in terms of trap-specific and/or time-specific covariates so that inferences about animal movements or behaviors could be made

These components added biological realism to the SCR model and provided accurate and precise estimates of population abundance and distribution.

The analysis of detections of *unmarked* individuals lies at the opposite end of the above spectrum. Detections of unmarked individuals provide the most challenging estimation problem, even though Chandler and Royle (2013) claimed to have solved this problem. Models for the analysis of Florida panther detections lie at an intermediate position along the spectrum. Although Florida panthers do not have natural marks for identifying individuals, each year a few individuals are fitted with GPS collars and these individuals can be detected in camera-trap surveys along with unmarked panthers. Therefore, we were interested also in developing spatial mark-resight (SMR) models to analyze the detections of *marked and unmarked* individuals (i.e., a partially marked population). Importantly, we sought to develop models that included the same components used in the SCR models of Dorazio and Karanth (2017) so that biologically realistic and accurate estimates of Florida panther distribution and abundance could be obtained.

2 METHODS

We relied primarily on simulation studies to assess the performance of the statistical models that we developed for analyzing various kinds of data. In these studies we simulated data based on the assumptions and parameter values of a prescribed statistical model. We then attempted to fit this model (that is, to estimate its parameters) using the simulated data. Simulation studies are a time-honored approach used in model development and assessment. They are motivated by asymptotic properties of maximum-likelihood and Bayesian estimators (Royle and Dorazio, 2008), wherein the average value of a parameter estimate converges to the (true) value that was used to simulate the data as the amount of information in the data grows.

Simulation studies therefore provide a method of evaluating the operating characteristics of a statistical model. Does the model perform "as advertised?" If not, why not? What are the conditions under which a model's parameters can be estimated accurately from a set of data? In this sense, the analysis of simulated data is a logical and useful antecedent to the analysis of real data.

Building upon the results of Chandler and Royle (2013) and Sollmann et al. (2013b), we used simulation studies to assess the performance of models that we developed for the analysis of three kinds of data: (1) detections of unmarked individuals, (2) resightings of marked individuals, and (3) resightings of marked individuals and detections of unmarked individuals. We describe the models of these data in the following sections.

2.1 Analysis of Detections of Unmarked Individuals

The assumptions of the SCR model of Dorazio and Karanth (2017) contain the biological realism that we wished to include in models of unmarked or partially marked populations. Therefore, we simulated data under the assumptions of the SCR model and then ignored the individual-level information in the

data. In other words, we simply added the numbers of trap-specific detections per individual among all individuals to obtain the total number of detections at each trap.

Without going into detail, we developed a statistical model to analyze the detections of unmarked individuals generated by the SCR model. We then used a wide range of parameter values to simulate detections of unmarked individuals (that is, we assumed different population densities, different detection rates, different levels of individual movement, etc.), and we observed a surprising result:

> Population abundance could not be estimated reliably from the simulated data, particularly if populations were composed of many individuals (i.e., a high density of individual activity centers).

This result was certainly unexpected given the apparent successes that had been reported by Chandler and Royle (2013). Therefore, to determine whether our findings were limited to our model or were perhaps more general, we decided to conduct an additional set of simulation studies. In these studies we simulated data using the modeling assumptions and the R code of Chandler and Royle (2013), and we estimated population abundance and other parameters of the model using the R code of Chandler and Royle (2013) (see S1 Supplement). To examine the estimation problems that we anticipated, we simulated data for two populations of unmarked individuals: a low-density population of $N = 45$ individuals, and a high-density population of $N = 450$ individuals. Each simulated population occupied a square (20×20) spatial domain, and individuals were potentially detected at each of 225 equally spaced traps placed in the middle of the spatial domain (Figure 1). Individuals of both populations shared the same baseline encounter rate and the same spatial extent of movement (parameterized by $\lambda_0 = 0.5$ and $\sigma = 0.5$., respectively, in the notation of Chandler and Royle (2013)).

2.2 Analysis of Resightings of Marked Individuals

The resightings of individuals marked prior to a camera-trap survey provide individual-level information that can be informative of an individual's baseline detection rate, spatial extent of movements, and activity center. This holds true even if some of the marked individuals are not detected at any trap locations during the survey. In camera-trap surveys of Florida panthers, only a few individuals (4–6 panthers) are typically marked (GPS-collared) prior to each survey. Therefore, we conducted analyses of both simulated and actual resightings of only a few individuals to examine how much could be learned about population-level parameters from these data alone.

2.2.1 Simulated population resighted in one-dimensional spatial domain

We simulated a populuation of individuals living along a finite, one-dimensional spatial domain $B = [-15, 15]$. We assumed that the limiting, expected density of individuals $\lambda(s)$ at any location $s \in B$ depended on the value of single, spatially varying covariate $v(s)$ as follows:

$$\lambda(s) = \exp(\beta_0 + \beta_1 v(s))$$

where β_0 and β_1 are parameters of known value (-1 and 2, respectively). In our simulated population $v(s)$ declined linearly with s, so $\lambda(s)$ declined exponentially with s (Figure 2).

We assumed that $\lambda(s)$ was the intensity of a Poisson point process over B so that the expected number of individuals living in B equaled $\Lambda(B) = \int_B \lambda(s)\,\mathrm{d}s$. A realization of this point process yields a population of N individuals whose activity centers are denoted by $s_1, s_2, \ldots, s_N$. To specify a simple model for the detection of these individuals, we assumed that during $T = 10$ units of time each

individual was exposed to an array of $K = 201$ evenly spaced traps within the interval $[-10, 10]$. We further assumed that the number of detections y_{ik} of the ith individual in trap k depended on the distance between that individual's activity center s_i and the trap's location x_k as follows:

$$y_{ik}|s_i \sim \text{Poisson}\left(T\phi_0 \exp\left(-\frac{||s_i - x_k||^2}{2\sigma^2}\right)\right) \quad (1)$$

where ϕ_0 denotes the baseline detection rate of an individual and where the scale parameter σ specifies the spatial extent of an individual's movements around its activity center. For each simulated population we assumed $\phi_0 = 0.5$ and $\sigma = 0.2$. Figure 3 illustrates the activity centers of a typical simulated population and the expected number of detections of all individuals along the trapping array.

From the simulated population of N individuals, we randomly selected $m = 6$ individuals to be marked and potentially resighted along the array of K traps. At the end of the survey the detections of these individuals were recorded in a $m \times K$ matrix $\boldsymbol{y}_{(1:m)}$ of individual- and trap-specific counts. We cannot expect to learn much about the spatial variation in density of individual activity centers from the detections of only $m = 6$ individuals; therefore, we fit a relatively simple model to the resightings data where the activity centers were assumed to be uniformly distributed in B and where the number of detections followed the Poisson distribution given in Eq. 1. We estimated the parameters of this model (i.e., ϕ_0 and σ) by maximizing the following likelihood function:

$$L(\phi_0, \sigma|\boldsymbol{y}_{1:m}) = \prod_{i=1}^{m} \int_B [s_i] \prod_{k=1}^{K} [y_{ik}|s_i] \mathrm{d}s_i$$

wherein bracket notation is used to specify the probability density functions of s_i and y_{ik}. We also estimated the activity center s_i of the ith resighted individual using a conditional distribution with the following probability density function:

$$[s_i|y_{i1}, \ldots, y_{iK}, \hat{\phi}_0, \hat{\sigma}] = \frac{[s_i] \prod_{k=1}^{K} [y_{ik}|s_i]}{\int_B [s] \prod_{k=1}^{K} [y_{ik}|s] \mathrm{d}s}$$

which conditions on the parameter estimates $\hat{\phi}_0$ and $\hat{\sigma}$. These estimates of s_i are sometimes referred to as empirical Bayes estimates because the conditional distribution is derived using Bayes' rule.

We include R code for simulating the data and for fitting the model to these data in S2 Supplement.

2.2.2 Florida panthers resighted in Big Cypress National Preserve

We analyzed the resightings data of 6 Florida panthers that were marked (GPS collared) near the Addition Lands Unit of Big Cypress National Preserve in 2014 and detected in that year's camera-trap survey. Although 8 panthers were actually marked, two individuals (ID Numbers 224 and 231) were thought to be transients and were excluded from our analysis. The study area and sampling methods are described in detail in our report for Phase 1 of the project.

We fitted the same model used to analyze simulated resightings data except that we considered a two-dimensional spatial domain and an array of only $K = 50$ camera traps. In addition, we used the Bayesian method of analysis instead of a maximum-likelihood approach. The Bayesian method was selected as a computational expedient. We include R code for reading the panther data and for fitting the model to these data in S3 Supplement.

2.3 Analysis of Resightings and Detections of Unmarked Individuals

Using the data-generating model described in Section 2.2.1, we simulated a population of individuals living along a finite, one-dimensional spatial domain $B = [-15, 15]$. We used the same parameter values used earlier except for $\boldsymbol{\beta}$, which we assigned the following value: $\boldsymbol{\beta} = (1, 1)'$. This value implied a larger population with an expected size of about 129 individuals. We randomly selected $m = 6$ individuals from the simulated population to be marked and potentially resighted along the array of K traps. At the end of the survey the detections of these individuals were recorded in a $m \times K$ matrix $\boldsymbol{y}_{(1:m)}$ of individual- and trap-specific counts. In addition, we recorded the number of detections of unmarked individuals in each trap. Let $\tilde{\boldsymbol{y}}$ denote the K-vector of counts containing the detections of these unmarked individuals.

To analyze the resightings and the detections of unmarked individuals, we adopted the approach used by Chandler and Royle (2013) but we developed a different model. Specifically, we developed a spatial capture-recapture (SCR) model that could be used to analyze a set of *latent* individual-level captures associated with the unknown number of unmarked individuals. The set of latent captures specified in this model were analyzed together with the *observed* resightings of each marked individual.

2.3.1 A spatial mark-resight (SMR) model

To specify the SMR model, we first describe a model of resightings of m marked individuals. This model is essentially the same as that used earlier (Section 2.2.1), except that we retain the activity centers of each individual as formal parameters to be estimated. We assumed that the number and locations of the N activity centers are outcomes of an inhomogenous, Poisson process with intensity function $\lambda(s) = \exp(\beta_0 + \beta_1 v(s))$; therefore, the conditional density of s is proportional to $\lambda(s)/\Lambda(B)$, and the likelihood function for the resightings data is:

$$[\boldsymbol{y}_{(1:m)}, \boldsymbol{s}_{(1:m)} \mid \phi_0, \sigma, \boldsymbol{\beta}] = m! \prod_{i=1}^{m} [s_i] \prod_{k=1}^{K} [y_{ik}|s_i] \tag{2}$$

where $[s_i] = \lambda(s_i)/\Lambda(B)$ and where $[y_{ik}|s_i]$ denotes the probability mass function of the Poisson distribution given in Eq. 1.

Some of the $N - m$ unmarked individuals in the population have contributed to $\tilde{\boldsymbol{y}}$, the vector of trap-specific detection frequencies of unmarked individuals. However, the size N of the population is not known. For the moment suppose counterfactually that individual-level information was observable for the $N - m$ unmarked individuals, and index these individuals by $u = 1, \ldots, U$ where $U = N - m$. This yields a $U \times K$ matrix of individual- and trap-specific detections y_{uk}. To estimate U, we augmented this matrix by an arbitrarily large number of all-zero rows and we expanded the SCR model to include a $M \times K$ matrix of augmented counts. This approach, developed by Royle and Dorazio (2012), is called parameter-expanded data augmentation.

Our model of the augmented counts is based on the following assumptions:

- $z_u \sim \text{Bernoulli}(\psi)$, where $\psi = (\Lambda(B) - m)/M$
- $[s_u] = \lambda(s_u)/\Lambda(B)$
- $y_{uk}|s_u, z_u \sim \text{Poisson}\left(z_u \, T\phi_0 \exp\left(-\frac{||s_u - x_k||^2}{2\sigma^2}\right)\right)$

In this model the unknown number of unmarked individuals U is a derived parameter that can be estimated as follows: $U = \sum_{i=1}^{M} z_i$. Let $\boldsymbol{y}_{(1:M)}$ denote the $M \times K$ matrix of augmented counts. The likelihood function for the model of these counts is:

$$[\boldsymbol{y}_{(1:M)}, \boldsymbol{z}, \boldsymbol{s} \mid \phi_0, \sigma, \boldsymbol{\beta}] = \left[\prod_{u=1}^{M} [z_u|\psi][s_u]\right] \times \left[\prod_{k=1}^{K}\prod_{u=1}^{M} [y_{uk}|z_u, s_u]\right] \tag{3}$$

where $\boldsymbol{z} = (z_1, \ldots, z_M)'$ and where $\boldsymbol{s} = (s_1, \ldots, s_M)'$.

Recall that $\boldsymbol{y}_{(1:M)}$, the matrix of individual-level counts, is actually *latent*, not observed. However, these counts are related to the observed counts $\tilde{\boldsymbol{y}} = (\tilde{y}_1, \ldots, \tilde{y}_K)'$ as follows: $\tilde{y}_k = \sum_{u=1}^{M} y_{uk}$. Furthermore, the assumptions of the model of augmented counts imply

$$\tilde{y}_k|\boldsymbol{z}, \boldsymbol{s} \sim \text{Poisson}\left(\sum_{u=1}^{M} z_u \, T\phi_0 \exp\left(-\frac{||s_u - x_k||^2}{2\sigma^2}\right)\right)$$

This result provides an important connection between the observed vector of counts $\tilde{\boldsymbol{y}}$ and the latent matrix of counts $\boldsymbol{y}_{(1:M)}$. Specifically, the product in the second pair of square brackets on the right-hand side of Eq. 3 is a product of Poisson probabilities, and it is easily shown that for each value of k this product is mathematically equivalent to a product of Poisson and multinomial probability mass functions as follows:

$$\prod_{u=1}^{M} [y_{uk}|z_u, s_u] = [\tilde{y}_k|\boldsymbol{z}, \boldsymbol{s}] \; [y_{1k}, \ldots, y_{Mk}|\, \tilde{y}_k, \pi_1(\boldsymbol{z}, \boldsymbol{s}), \ldots, \pi_M(\boldsymbol{z}, \boldsymbol{s})]$$

where $[\tilde{y}_k|\boldsymbol{z}, \boldsymbol{s}]$ is the Poisson probability mass function and where the multinomial cell probability for the uth individual equals

$$\pi_u(\boldsymbol{z}, \boldsymbol{s}) = \frac{z_u \, \phi(s_u, x_k)}{\sum_{l=1}^{M} z_l \, \phi(s_l, x_k)}$$

where $\phi(s_u, x_k) = \exp\left(-\frac{||s_u - x_k||^2}{2\sigma^2}\right)$. This mathematical equivalence allows us to specify the following likelihood function, which includes *both* the latent matrix of counts and the observed vector of counts:

$$[\boldsymbol{y}_{(1:M)}, \tilde{\boldsymbol{y}}, \boldsymbol{z}, \boldsymbol{s} \mid \phi_0, \sigma, \boldsymbol{\beta}] = \left[\prod_{u=1}^{M} [z_u|\psi][s_u]\right] \times \left[\prod_{k=1}^{K} [\tilde{y}_k|\boldsymbol{z}, \boldsymbol{s}] \; [y_{1k}, \ldots, y_{Mk}|\, \tilde{y}_k, \pi_1(\boldsymbol{z}, \boldsymbol{s}), \ldots, \pi_M(\boldsymbol{z}, \boldsymbol{s})]\right] \tag{4}$$

To estimate the parameters of our SMR model of resightings and of detections of unmarked individuals, we use the likelihood functions from Eqs. 2 and 4 to form the following joint posterior density function:

$$\begin{aligned}[\boldsymbol{y}_{(1:M)}, \boldsymbol{z}, \boldsymbol{s}, \boldsymbol{s}_{(1:m)}, \phi_0, \sigma, \boldsymbol{\beta} \mid \tilde{\boldsymbol{y}}, \boldsymbol{y}_{(1:m)}] \quad &\propto \quad [\phi_0, \sigma, \boldsymbol{\beta}] \; [\boldsymbol{y}_{(1:M)}, \tilde{\boldsymbol{y}}, \boldsymbol{z}, \boldsymbol{s} \mid \phi_0, \sigma, \boldsymbol{\beta}] \\ &\quad \times [\boldsymbol{y}_{(1:m)}, \boldsymbol{s}_{(1:m)} \mid \phi_0, \sigma, \boldsymbol{\beta}]\end{aligned}$$

where $[\phi_0, \sigma, \boldsymbol{\beta}]$ specifies the prior probability density for the parameters ϕ_0, σ, and $\boldsymbol{\beta}$. (We omit the technical details of computing summaries of a posterior distribution with this density.)

3 RESULTS

3.1 Analysis of Unmarked Individuals

Our analysis of simulated data revealed a distinct difference between the parameter estimates associated with the two populations (i.e., between the low-density population of $N = 45$ individuals and the high-density population of $N = 450$ individuals). For the low-density population, trace plots of the Markov chains were only moderately autocorrelated and showed no signs of drift around the parameter space (Figure 4). In contrast, trace plots associated with the high-density population revealed extremely high autocorrelation that was not associated with transient behavior of the Markov chain.

We similarly obtained highly autocorrelated trace plots when attempting to fit our model of detections of unmarked individuals generated by the SCR model of Dorazio and Karanth (2017). However, the model of Chandler and Royle (2013) is *much* simpler and allowed us to identify the source of the estimation problem. We determined (with corroboration of additional simulation studies) that the levels of autocorrelation and drift of the Markov chain can be made arbitrarily high simply by increasing the number N and density of individuals in the population. Therefore, the parameters of Chandler and Royle's model appear to become unidentified with increases in the density of individual activity centers. In other words, although the number of detections of unmarked individuals increases with increases in population density, an analyst cannot determine whether the increased number of detections is attributed to a high detection rate of few individuals or to a low detection rate of many individuals. We can summarize our results with unmarked populations as follows:

> *It is not possible to estimate population abundance and distribution reliably if the density of individual activity centers is too high.*

Royle is aware of this estimation problem (personal communication), but the limitations of Chandler and Royle's (2013) model have never been described in the published literature. The simulation studies conducted by Chandler and Royle were limited to low-density populations of $N = 27$, 45, or 75 individuals. This relatively small range in population sizes may be the reason why Chandler and Royle overstated the applicability of their model of unmarked populations. Unfortunately, we spent several months of effort to discover this estimation problem.

3.2 Analysis of Resightings of Marked Individuals

3.2.1 Simulated population resighted in one-dimensional spatial domain

Of the 6 individuals selected from the simulated population, only 2 individuals were detected in the trapping array. One individual was detected 20 times, and the other was detected 21 times during the survey. Despite this outcome, the data provided reasonably accurate estimates of the baseline rate of detection ($\hat{\phi}_0 = 0.43$, 95% confidence interval = 0.30–0.62) and of the movement parameter ($\hat{\sigma} = 0.23$, 95% confidence interval = 0.18–0.29). The estimated distributions of the activity centers of the two detected individuals were quite accurate (Figure 5). All that can be inferred about the activity centers of the other 4 individuals is that they were located with uniform probability at all locations lying outside the trapping array.

We did not complete an extensive simulation study that included multiple populations and different parameter values. However, we analyzed many sets of simulated resightings data (not shown), and in each case we obtained results similar to those illustrated by our example data set.

3.2.2 Florida panthers resighted in Big Cypress National Preserve

All 6 panthers were detected in the camera-trap array with the following encounter statistics:

ID number	No. detections	No. camera locations
177	50	22
199	14	7
216	1	1
225	9	7
226	29	9
227	7	4

The posterior mean of the movement parameter σ was 4.5 km (95% credible interval = 3.8–5.4). The posterior mean of the baseline detection rate ϕ_0 was 0.52 panthers per 30 days (95% credible interval = 0.38–0.69). The posterior distributions of activity centers of the three panthers with the highest number of resightings are shown in Figure 6.

Our estimate of σ is similar to 4.45 km, an estimate computed for panthers detected within the Picayune Strand Restoration Project (PSRP) area (Sollmann et al., 2013a). However, our estimate of ϕ_0 is much higher than 0.09 panthers per 30 days, the estimated baseline detection rate of panthers within the PSRP area.

3.3 Analysis of Resightings and Detections of Unmarked Individuals

We simulated a population of $N = 150$ individuals, and 79 of these individuals were detected (at least once) in the trapping array. As expected, fitting a SCR model to the recaptures of these 79 individuals yielded parameter estimates that were similar to the values used to generate the data, as shown in the following table of estimated posterior means and percentiles:

Parameter	True value	Mean	2.5%	97.5%
σ	0.2	0.195	0.189	0.201
ϕ_0	0.5	0.530	0.501	0.561
β_0	1.0	1.044	0.768	1.288
β_1	1.0	1.121	0.816	1.460
N	150	152.2	126.0	189.0

However, our primary interest was focused on fitting the SMR data. Four of the 6 individuals selected from the simulated population were detected in the trapping array with the following total numbers of detections per individual: 37, 28, 33, and 19. The numbers of detections per trap of unmarked individuals ranged from zero to 35 (Figure 7) and were highest in regions of the spatial domain that had the highest density of individuals.

Unfortunately, when analyzing these SMR data we were not able to achieve results comparable to those obtained in the analysis of recaptures. Although the Markov chains for σ and ϕ_0 were not highly autocorrelated and were centered near their true (data-generating) values (Figure 8), the Markov chains for β_0 and β_1 were strongly autocorrelated and drifted in the parameter space. (Drift was more evident in longer chains (not shown).) In addition, the Markov chain for β_0 was relatively far from the true (data-generating) value of this parameter (i.e., $\beta_0 = 1$), and the Markov chain for abundance N contained values much smaller than the actual population size.

We did not complete an extensive simulation study that included multiple populations and different parameter values. However, we analyzed many sets of simulated SMR data (not shown), and in each

case we obtained results that were either similar or worse than those illustrated by our example data set. Results were particularly poor when we attempted to analyze data from small populations where densities were relatively low over much of the spatial domain.

4 DISCUSSION

Our plans to develop a coherent analytical framework for the analysis of populations of either completely marked, partially marked, or unmarked individuals were not successful. Our minimal objective was to develop a statistical model that could be used to estimate spatial differences in density of individual activity centers as a function of one or more spatially varying covariates measured throughout the breeding range of Florida panthers. Unfortunately, none of the models that we developed for the analysis of unmarked or partially marked populations was able to achieve this objective.

Our analyses of unmarked populations revealed the rather shocking finding that *it is not possible to estimate population abundance and distribution reliably if the density of individual activity centers is too high.* To our knowledge, this result has never been reported in the published literature (Chandler and Royle, 2013; Sollmann et al., 2013a,b; Royle et al., 2014). Although this literature includes several simulation studies, the studies are limited to low-density populations. By failing to describe the estimation problems that we encountered, the authors of these studies have overstated the utility of their models. Furthermore, the extent of their model's applicability has not been adequately explored using either theoretical or empirical methods.

We had expected better results from the joint analysis of resightings and detections of unmarked individuals. For example, our analyses of only resightings (simulated or real) from $m = 6$ individuals confirmed that much can be learned about an individual's baseline rate of detection, spatial extent of movements, and even activity center. However, the resightings of only 6 individuals provides relatively little information about spatial differences in the density of individual activity centers. We had hoped that our SMR model for the joint analysis of resightings and detections of unmarked individuals could leverage the information in the resightings data to help inform other parameters of the model ($\boldsymbol{\beta}$) that specify spatial differences in the density of individual activity centers. Unfortunately, our analyses of simulated SMR data suggest that the detections of unmarked individuals do not contain sufficient information to estimate $\boldsymbol{\beta}$ accurately. The absence of individual-level information appears to be a serious impediment to learning about spatial differences in the density of individual activity centers.

5 RECOMMENDATIONS

The SMR model of Sollmann et al. (2013a), which was used in Phase 1 of our project, can provide an accurate – though not necessarily precise – estimate of average panther density during a camera-trap survey. We therefore recommmend this model and include R code for fitting the model to Florida panther SMR data (see S4 Supplement). At the very least, this model provides estimates of abundance and density of Florida panthers in the vicinity of the camera-trap survey.

The enormous inferential benefits of obtaining individual-level information about Florida panthers are irrefutable. The cost of this information (that is, of locating, marking and monitoring individually-marked panthers) may be high but there is no better way to learn how panther density varies spatially and how individual panthers move and utilize different habitats across their breeding range. Collecting individual-level information for only a handful of panthers each year seems unlikely to yield accurate and precise estimates of Florida panther abundance throughout its breeding range. Increasing the

number of panthers marked each near is needed to obtain any substantial improvement in estimates of Florida panther density based on SMR models.

SUPPLEMENTAL INFORMATION

S1 Supplement R code used in simulation study of Chandler and Royle's (2013) model of detections of unmarked individuals.

S2 Supplement R code for fitting our model of resightings for a simulated population of partially marked individuals.

S3 Supplement R code for fitting our model of resightings of Florida panthers marked in the Addition Lands of Big Cypress National Park during 2014.

S4 Supplement R code for fitting model of Sollmann et al. (2013a) to a partially marked Florida panther population in the Addition Lands Unit of Big Cypress National Preserve during 2014.

DISCLAIMERS

1. This report was prepared under contract in a grant to the U.S. Geological Survey (USGS). Opinions and conclusions expressed herein do not necessarily represent those of the USGS.
2. Any use of trade, firm, or product names is for descriptive purposes only and does not imply endorsement by the U.S. Government.
3. This software is preliminary or provisional and is subject to revision. It is being provided to meet the need for timely best science. The software has not received final approval by the U.S. Geological Survey (USGS). No warranty, expressed or implied, is made by the USGS or the U.S. Government as to the functionality of the software and related material nor shall the fact of release constitute any such warranty. The software is provided on the condition that neither the USGS nor the U.S. Government shall be held liable for any damages resulting from the authorized or unauthorized use of the software.

References

Chandler, R. B. and Royle, J. A. (2013). Spatially-explicit models for inference about density in unmarked or partially marked populations. *Annals of Applied Statistics*, 7:936–954.

Dorazio, R. M. and Karanth, K. U. (2017). A hierarchical model for estimating the spatial distribution and abundance of animals detected by continuous-time recorders. *PLoS One*, in review.

Royle, J. A., Chandler, R. B., Sollmann, R., and Gardner, B. (2014). *Spatial capture-recapture*. Academic Press, Amsterdam.

Royle, J. A. and Dorazio, R. M. (2008). *Hierarchical modeling and inference in ecology*. Academic Press, Amsterdam.

Royle, J. A. and Dorazio, R. M. (2012). Parameter-expanded data augmentation for Bayesian analysis of capture-recapture models. *Journal of Ornithology*, 152:S521–S537.

Sollmann, R., Gardner, B., Chandler, R. B., Shindle, D. B., Onorato, D. P., Royle, J. A., and O'Connell, A. F. (2013a). Using multiple data sources provides density estimates for endangered Florida panther. *Journal of Applied Ecology*, 50:961–968.

Sollmann, R., Gardner, B., Parsons, A. W., Stocking, J. J., McClintock, B. T., Simons, T. R., Pollock, K. H., and O'Connell, A. (2013b). A spatial mark-resight model augmented with telemetry data. *Ecology*, 94:553–559.

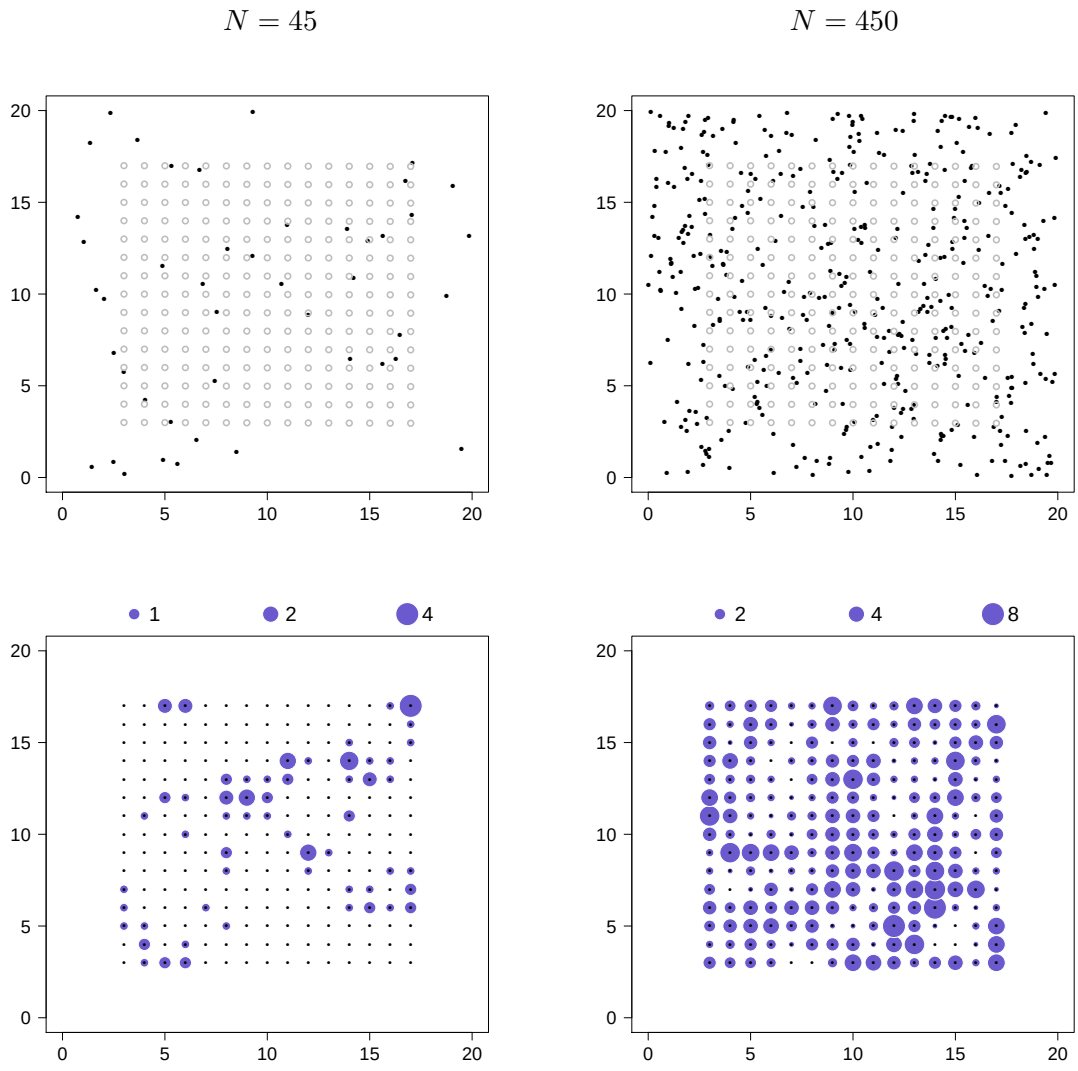

Figure 1: Spatial distribution of individual activity centers (upper panels) and of number of detections (lower panels) for two populations simulated using the model of Chandler and Royle (2013). Trap locations are indicated by open circles in upper panels. One population was composed of $N = 45$ individuals (left panels), whereas the other population was composed of $N = 450$ individuals (right panels).

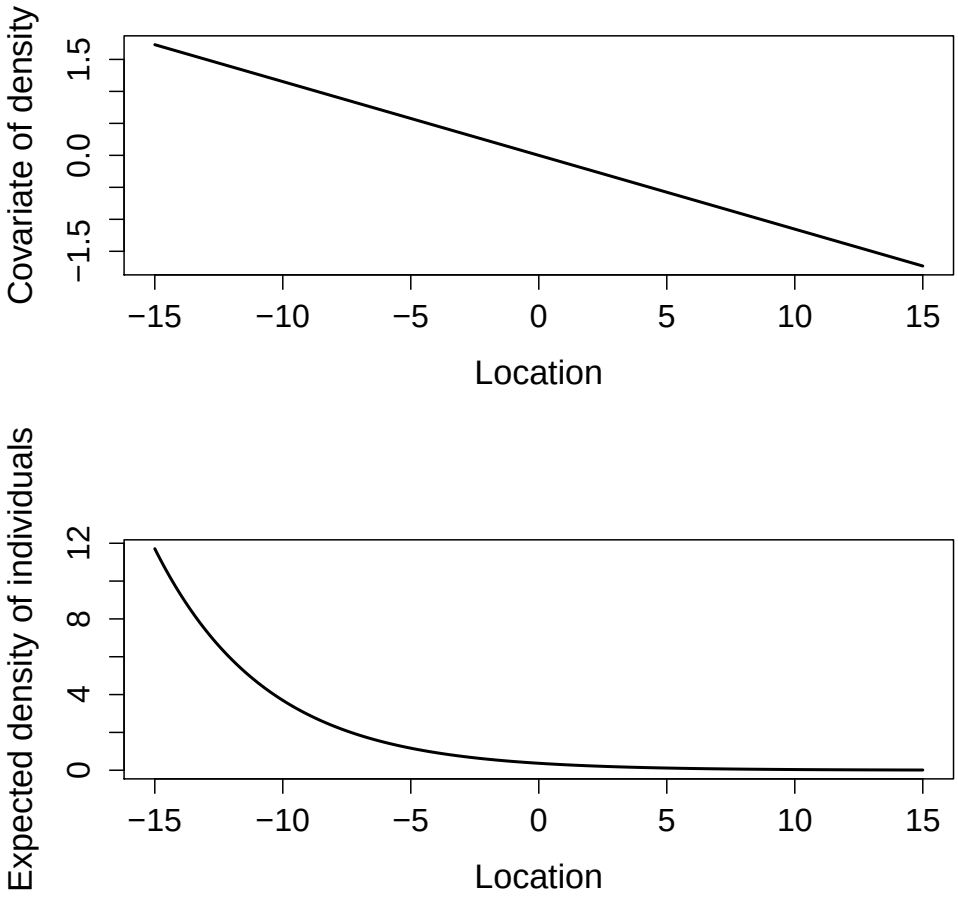

Figure 2: Spatially varying covariate (upper panel) and expected density of individuals (lower panel) used to simulate the distribution of individual activity centers in a one-dimensional spatial domain.

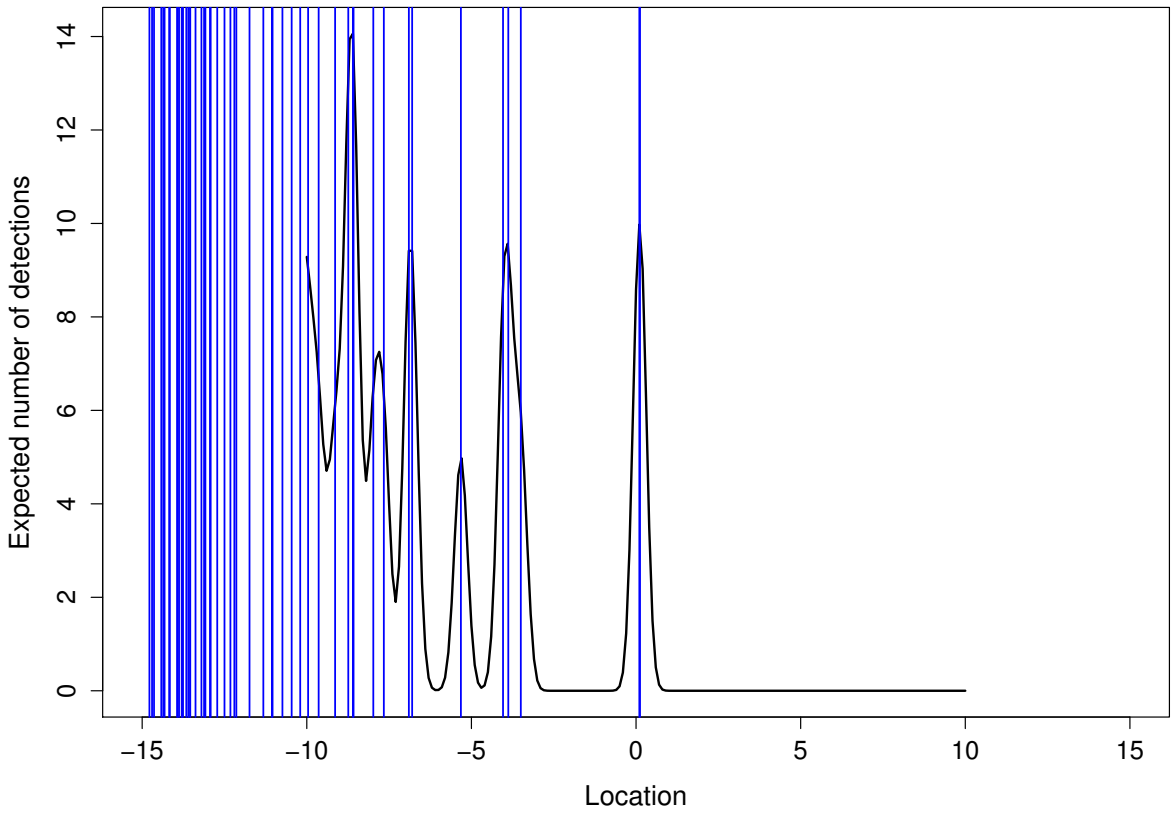

Figure 3: Expected number of detections (black line) as a function of location for all individuals in the simulated population. A vertical blue line indicates the activity center of a single individual.

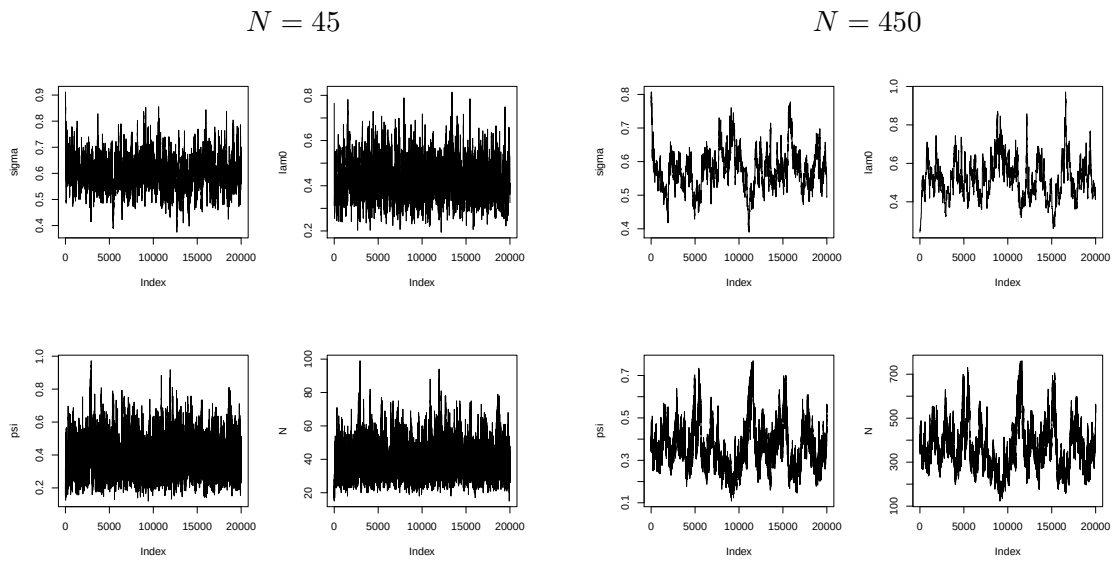

Figure 4: Trace plots of Markov chains obtained while fitting the model of Chandler and Royle (2013) to the detections of unmarked individuals from each of two populations. One population was composed of $N = 45$ individuals (left panels), whereas the other population was composed of $N = 450$ individuals (right panels).

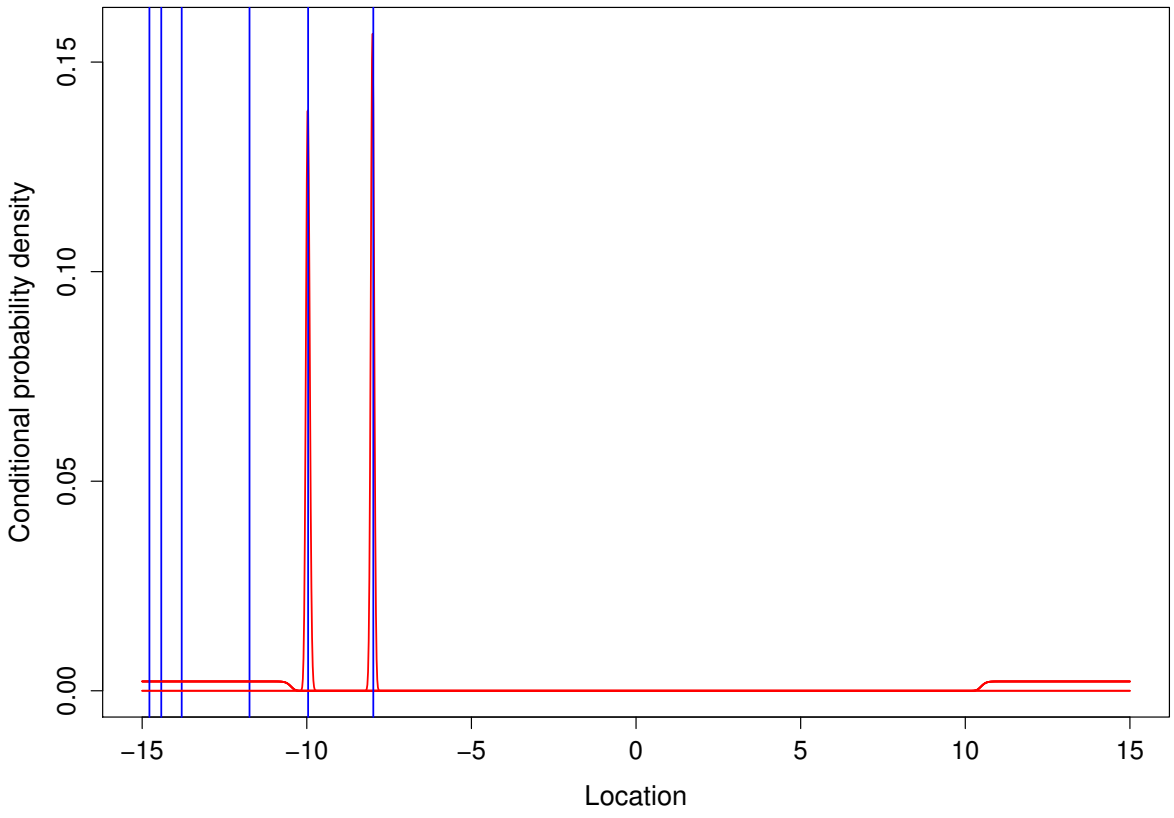

Figure 5: Estimates of the conditional distribution of activity centers for each resighted individual in the simulated population. A vertical blue line indicates the activity center of a single individual.

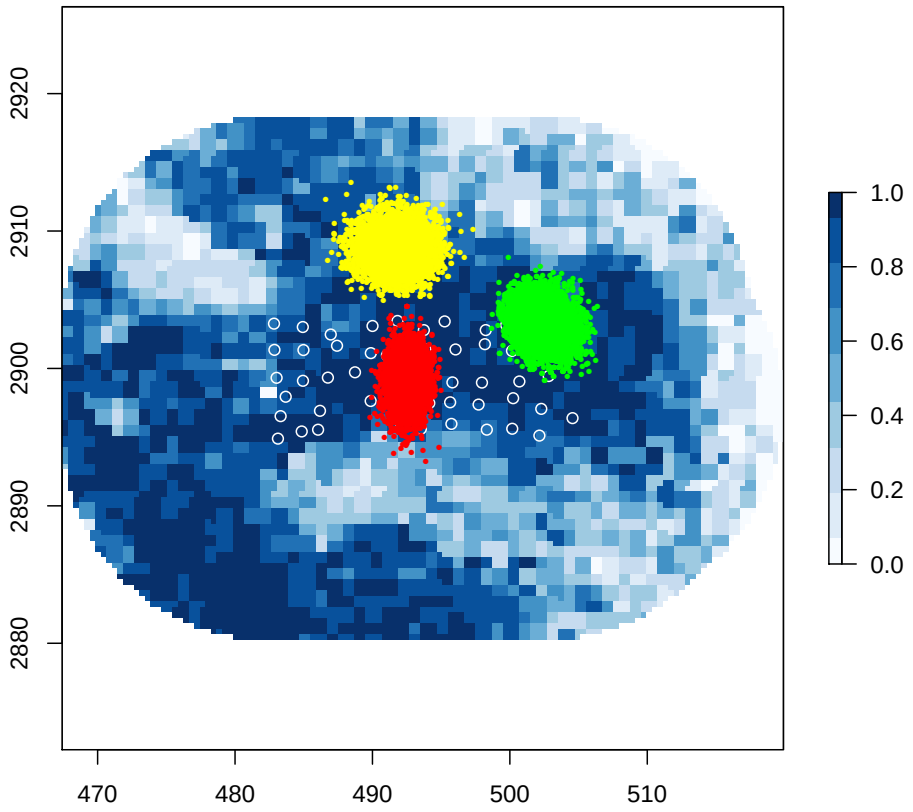

Figure 6: Estimated posterior distribution of activity centers of 3 collared Florida panthers (indicated by red (ID 177), yellow (ID 199), and green (ID 226)) in the Addition Lands Unit of Big Cypress National Preserve. Camera trap locations are indicated by white circles. Blue color scale indicates magnitude of Frakes score, an index of panther habitat.

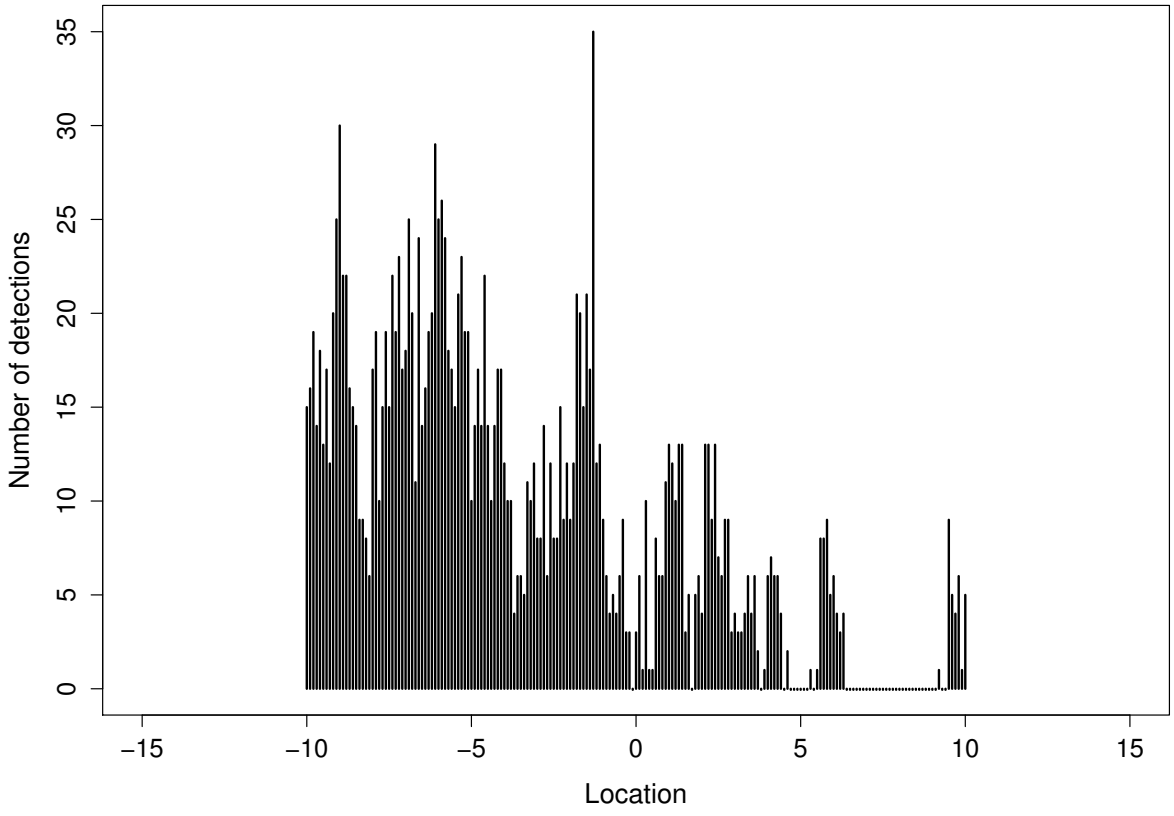

Figure 7: Number of detections of unmarked individuals per trap in a simulated population as a function of trap location.

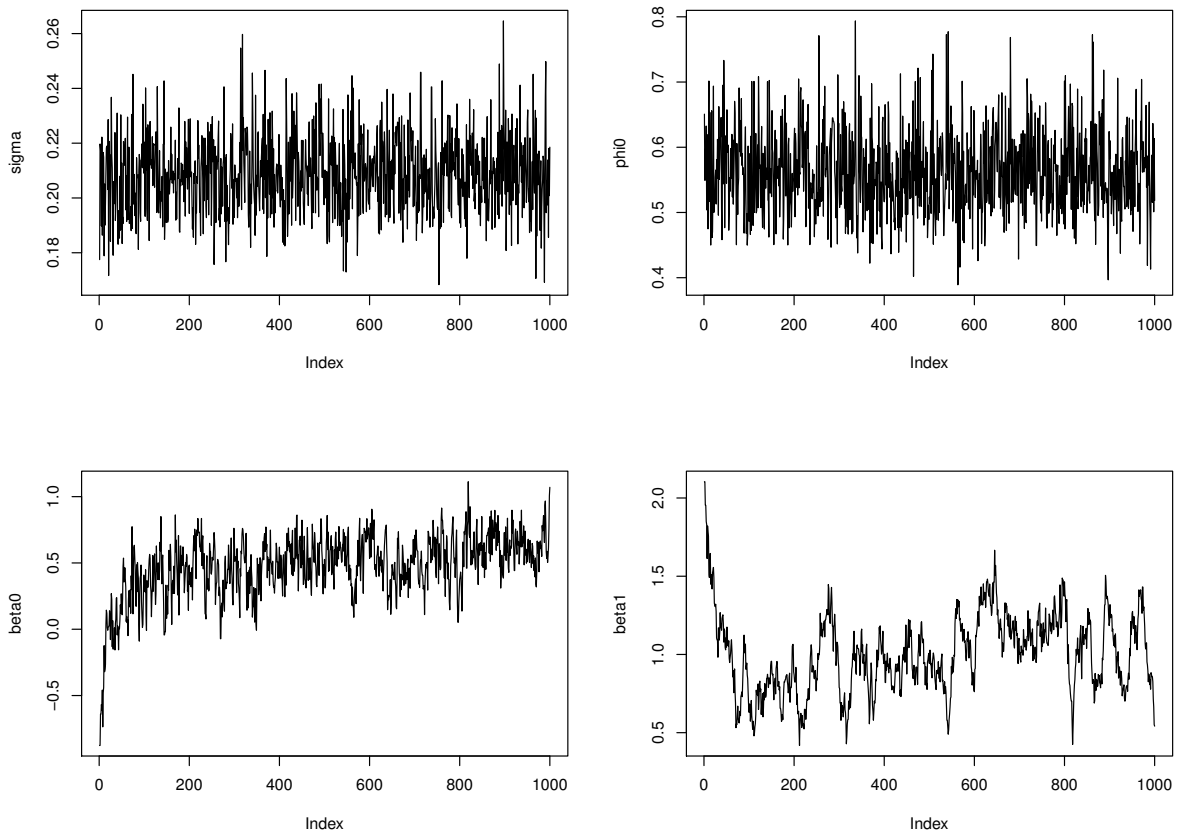

Figure 8: Trace plots of Markov chains obtained while fitting the SMR model to resightings and detections of individuals from a simulated population.